MICROSTRUCTURE AND CORROSION BEHAVIOR OF 70Cu-30Ni WELDED PIPE①

Wang, Jihui Jiang, Xiaoxia Li, Shizhuo
Institute of Metal Research, Chinese Academy of Sciences, Shengyang 110015

ABSTRACT The microstructure and corrosion behavior of 70Cu-30Ni welded pipe were investigated by EMPA, SEM, immersion test and electrochemical method. The results showed that: (1) with the process of drawing and annealing, the composition and microstructure tend to uniform; (2) the corrosion rate of heat affected zone is greater than that of base material; (3) the corrosion rate of welded pipe is about the same as that of seamless pipe.
Key words: cupronickel alloy welding corrosion behavior

1 INTRODUCTION

70Cu-30Ni alloy is widely used as heat exchange material in the condenser tube, the microstructure and corrosion behavior have been investigated by many scientists. It's well known the high corrosion resistance of this alloy[1-3].

In the past, 70Cu-30Ni condenser tube was usually seamless pipe made by extruding and rolling. The product process was complicated and expensive; Now engineers of many countries are trying to make welded pipe by welding. Because the composition and microstructure of welding joints are different from base material, the corrosion behavior of welding joints may become the decisive factor which determines the lifetime of condenser tube. In this paper, the microstructure and corrosion behavior of seamless and welded pipe of 70Cu-30Ni alloy will be investigated.

2 EXPERIMENTAL

2.1 *Material*

The composition of 70Cu-30Ni alloy (wt.-%) was Ni 30.10, Fe 0.94, Mn 0.85, Si 0.15, P 0.006, Pb 0.02 and Cu balance. The seamless pipe $d23$ mm $\times$ $\delta 0.85$ mm (δ - wall thickness) was made by the 70Cu-30Ni extruding ingot casting into $d60$ mm $\times$ 6 mm, and then six times rolling and annealing. The fabricating process of welded pipe was following: firstly welded the 125 mm $\times$ $\delta 1.2$ mm plate into $d40$ mm $\times$ $\delta 1.2$ mm pipe by high frequency welding machine, then drew and annealed three times into $d25$ mm $\times$ $\delta 0.9$ mm after 30 min annealing at 840 ℃, finally drawn into $d23$ mm $\times$ $\delta 0.85$ mm and annealed at 650 ℃ for 30 min.

In order to observe the change of microstructure and properties in the fabricating process, $d40$ mm $\times$ $\delta 1.2$ mm, $d25$ mm $\times$ $\delta 0.9$ mm, $d23$ mm $\times$ $\delta 0.85$ mm welded pipe and $d23$ mm $\times$ $\delta 0.85$ mm seamless pipe were chosen. By comparison of different pipe and different parts of the same welded pipe, the size of specimen was: (1) Pipe: $d40$ mm $\times$ $\delta 1.2$ mm $\times$ 14.0 mm (length), $d25$ mm $\times$ $\delta 0.9$ mm $\times$ 23 mm, $d23$ mm $\times$ $\delta 0.85$ mm $\times$ 25 mm (welded, seamless); (2) Base material (BM) and welding joints (WM): 30 mm in length, 20 mm in width. All speciments were grounded by abrasive paper, polished, and then cleaned with water and acetone for degreasing.

2.2 *Test Methods*

The microhardness of different parts of welded pipe was measured by micro-sclerome-

① Received Dec. 24, 1994

ter; the compositions of pipes were analysed by electron micro-probe (EMPA). The corrosion rate was measured at 60 ± 2 ℃ in 3.5 wt.-% NaCl and 25 g $FeCl_3 \cdot 6H_2O$ + 100 mL HCl/L solution by immersion test. The morphology of welded pipe after corrosion was observed by SEM and microscope.

The polarization curves of different pipe and different parts of the same welded pipe in 3.5 wt.-% NaCl solution at room temperature were determined by using the dynamic potential method with a sweep speed of 0.5 mV/s, a saturated calomel electrode (SCE) was used as the reference electrode.

3 RESULTS

3.1 *Microstructure and Composition of Welded Pipe*

Fig. 1, Table 1 and Fig. 2 are the microstructure, composition and element distribution of welded pipe. It can be seen that with the process of drawing, the width of welds, grain size and the width of grain boundary decrease, the composition difference between the welds and base material (consists of Ni and Cu) decreases. The welding joint of *d*23 mm welded pipe can hardly be seen, the composition of *d*23 mm welds is almost the same as that of base material. For the welding joint of *d*40 mm welded pipe in special, the heat affected zone (HAZ) has the large grain and broaden grain boundary because of the heat cycle of welding (Fig. 1).

Table 1 Composition of welding joints (wt.-%)

Specimen		Cu	Ni	Fe	Mn
d 40 mm	BM	68.34	30.06	0.78	0.84
	WM	60.58	37.63	1.05	0.74
d 25 mm	BM	68.00	30.38	0.85	0.77
	WM	63.72	34.36	1.05	0.87
d 23 mm	BM	68.63	29.48	1.04	0.85
	WM	68.14	29.95	0.98	0.84

3.2 *Microhardness of Welded Pipe*

Table 2 lists the microhardness of different welded pipe and different weld parts. It can be seen that the difference of microhardness among WM, HAZ and BM decreases with the process of drawing. For one given welded pipe, because of the large grain and broaden grain boundary in HAZ, the microhardness of HAZ is obviously less than that of BM. The microhardness of *d*23 mm seamless pipe is different from that of *d*23 mm welded pipe because of the different process.

3.3 *Immersion Test and Morphology After Corrosion*

Table 3 is the corrosion rate of welded pipes immersed in 3.5 wt.-% NaCl solution, 200 h and $FeCl_3$ + HCl solution, 72h. In 3.5 wt.-% NaCl solution, From *d*40 mm, *d*25 mm

Fig. 1 Microstructure of welded pipe
(a)— *d* 40 mm; (b)— *d* 25 mm; (c)— *d* 23 mm

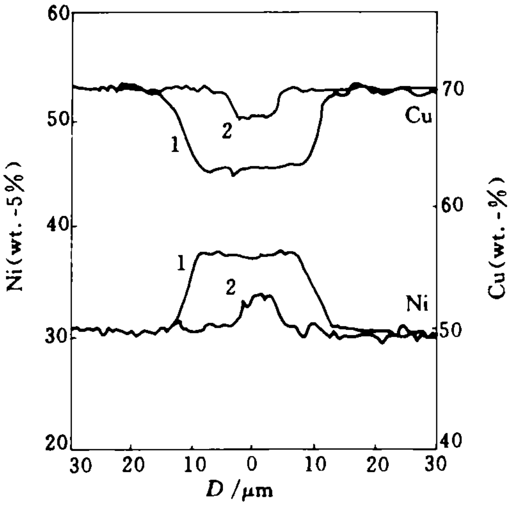

Fig. 2 Distribution of Ni and Cu in the welding joints

(1)— *d* 40 mm; (2)— *d* 25 mm; *D* —grain size of weld

Table 2 Microhardness of different pipes (Hv)

Specimen	BM	HAZ	WM
d 40 mm (Welded)	204.8	76.7	98.0
d 25 mm (Welded)	206.5	152.4	239.3
d 23 mm (Welded)	204.5	200.2	214.5
d 23 mm (Seamless)	137.4	—	—

and *d*23 mm (welded) to *d*23 mm (seamless), the corrosion rate of pipe and WM decrease; the corrosion rate of WM is larger than that of BM and that of the same pipe. The corrosion rate of *d*23 mm welded pipe is slightly larger than that of *d*23 mm seamless pipe; the corrosion rates of all BM is almost the same. Because the corrosion rate in 3.5 wt.-% NaCl solution is very small, the difference between WM and BM can hardly be distinguished by microscope and SEM. In $FeCl_3$ + HCl solution, the corrosion rate decreases from *d*40 mm, *d*25 mm and *d*23 mm (welded) to *d*23 mm (seamless); the corrosion rate of pipe and WM decrease in order, the corrosion rates of all BM are about the same; the corrosion rate of WM is larger than that of BM and pipe. The corrosion rate of *d*23 mm (welded) is slightly larger than that of *d*23 mm (seamless) pipe.

Fig. 3 is the surface morphology of welded pipes in $FeCl_3$ + HCl solution. It can be seen that there is a deep corrosion pit in the heat affected zone. It is proved that the corrosion rate of HAZ is larger than that of BM. From the section morphology (Fig. 4), the same conclusion can be obtained. After 108 h corrosion immersed *d*40 mm pipe and WM specimen in $FeCl_3$ + HCl solution, the welds was corroded away, the welds of *d*25 mm pipe was also corroded away in some area.

The maximum depth of WM of 190 μm, 72 μm and 23 μm are, respectively, related to BM of *d*40 mm, *d*25 mm and *d*23 mm welded pipe immersed in $FeCl_3$ + HCl solution for 36 h. From *d*40 mm to *d*23 mm (welded) pipe, the maximum depth decreases from 190 μm to 23 μm.

3.4 *Electrochemical Test*

Table 3 Corrosion rate of pipes in 3.5 wt.-% NaCl and $FeCl_3$+HCl solutions

Specimen	3.5 wt.-% NaCl, 200 h/10^{-3} mm·a^{-1}			$FeCl_3$+HCl, 72 h/mm·a^{-1}		
	Pipe	BM	WM	Pipe	BM	WM
d 23 mm (Seamless)	29.52	29.52	—	18.30	18.30	—
d 23 mm (Welded)	30.01	29.32	32.37	18.99	18.30	19.38
d 25 mm (Welded)	32.08	29.72	32.47	19.48	18.50	20.47
d 40 mm (Welded)	33.95	30.21	34.93	20.86	18.99	21.16

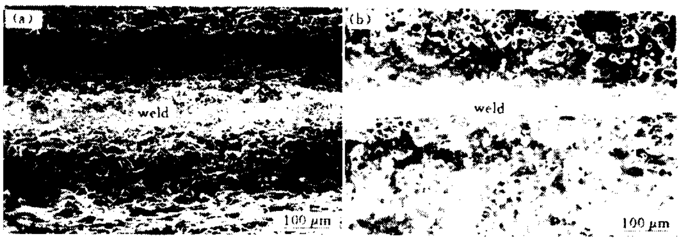

Fig. 3 Surface morphology of welded pipe in $FeCl_3$+HCl solution, 36 h
(a)— *d* 40 mm; (b)— *d* 23 mm

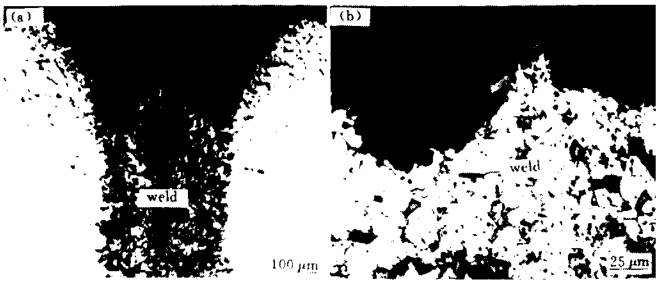

Fig. 4 Section morphology of welded pipe in $FeCl_3$+HCl solution, 36 h
(a)— *d* 40 mm; (b)— *d* 25 mm

Table 4 is the corrosion potential and corrosion current density of pipes in 3.5 wt.-% NaCl solution. The corrosion potential of *d*40 mm, *d*25 mm, and *d*23 mm (welded) are almost the same; the corrosion potential of *d*23 mm (welded) is more negative than that of *d*23 mm (seamless). The corrosion current density decreases from *d*40 mm, *d*25 mm and *d*23 mm (welded) to *d*23 mm (seamless); the corrosion current density of WM is larger than that of BM of the same pipe.

Table 4 Corrosion potential and current density in 3.5 wt.-% NaCl solution

Specimen	E_{Corr} /mV_{SCE}		I_{Corr} /$\mu A \cdot cm^{-2}$	
	BM	WM	BM	WM
d 23 mm (Seamless)	−159	—	10.2	—
d 23 mm (Welded)	−190	−184	24.87	28.40
d 25 mm (Welded)	−195	−186	36.70	39.89
d 40 mm (Welded)	−199	−192	39.90	44.20

Fig. 5 was the polarization curves of *d*23 mm (welded) and *d*23 mm (seamless) pipe. It shows that the corrosion potential of *d*23 mm (welded) is more negative than that of *d*23 mm (seamless), the corrosion current density of *d* 23 (welded) is larger than that of *d*23 mm (seamless).

4 DISCUSSION

After several drawing of welded pipe, the deformation increases. Diffusing and recrystallizing during the annealing at 650 ℃, the welded pipe tends to have the fine grain and fine grain boundary, the microstructure, composition and microhardness of welded parts are finally the same as those of BM.

Table 5 is the composition of grain and grain boundary of *d*40 mm HAZ. In the grain boundary of HAZ, the content of Ni is less than that of grain and BM, the contents of P, Pb are larger than those of grain. This result is the same as Savage's conclusion[4, 5]. It is these element's segregation that the melting point of grain boundary decreases and the grain boundary is broadened.

In ordinary circumstances, the heterogeneity of the microstructure would result in micro-electrochemical heterogeneity, produce micro electric cell, and then accelerate the corrosion loss of materials. For welding joints, the welded part, especially the heat affected zone with large grain, broad grain boundary and heterogeneity of composition, is the anode related to the base material. So the corrosion rate of welded parts is obviously larger than that of BM under the general corrosion of pipe.

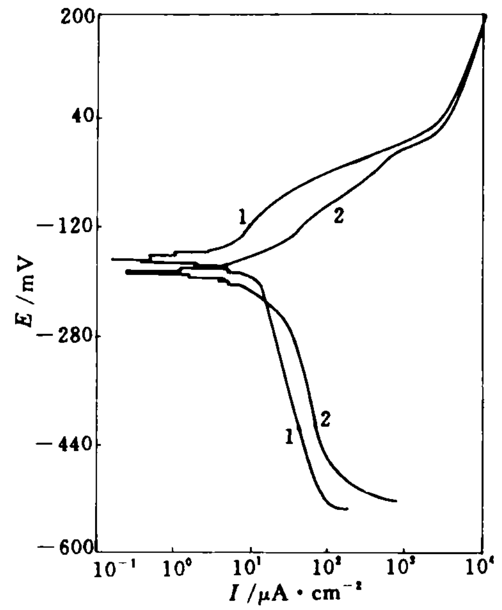

Fig. 5 Polarization curves of pipes *d* 23 mm
1— *d* 23 mm welds; 2— *d* 23 mm seamless

Table 5 Composition of grain and grain boundary of *d* 40 mm HAZ(wt. -%)

Specimen	Ni	Fe	Mn	P	Pb	Cu
Grain boundary	29.29	0.71	0.98	0.015	0.06	68.94
Grain	31.74	0.79	0.88	0.007	0.03	66.54

With the process of drawing and annealing, the microstructure of welding joint tends to uniform, the difference between HAZ and BM decreases, eventually disappears, thus the maximum depth of HAZ decreases.

5 CONCLUSION

(1) With the process of drawing and annealing, the composition and microstructure of welded pipe tend to uniform.

(2) In 3.5 wt. -% NaCl solution, the corrosion rate of welded pipe decreases with the process of drawing and annealing. The corrosion rate of *d*23 mm welded pipe is about the same as that of *d*23 mm seamless pipe.

(3) In $FeCl_3$+HCl solution, the general corrosion is occurred in the welded pipe, but the corrosion rate of HAZ is greater than that of BM.

REFERENCES

1 Al-Hajji, J N; Rede, M R. Corrosion, 1993, 49 (10): 809.
2 Tuthill, H A. Materials Performance, 1987, 26 (8): 12.
3 Syrett, B C; Roit, R L. Materials Performance, 1983, 22(2): 44.
4 Savage, W F *et al.* Welding Journal, 1976, 55(6): 165.
5 Savage, W F *et al.* Welding Journal, 1976, 55(7): 181.